doi: 10.17221/73/2017-VETMED

Contrast-enhanced computed tomography of the liver, gall bladder and urogenital tract in female red-eared terrapins (*Trachemys scripta elegans*)

V. Sochorcova[1]*, P. Proks[2], E. Cermakova[1], Z. Knotek[1]

[1]Avian and Exotic Animal Clinic, Faculty of Veterinary Medicine, University of Veterinary and Pharmaceutical Sciences Brno, Brno, Czech Republic

[2]Small Animal Clinic, Faculty of Veterinary Medicine, University of Veterinary and Pharmaceutical Sciences Brno, Brno, Czech Republic

*Corresponding author: sochorcova.veronika@seznam.cz

ABSTRACT: The aim of the present study was to evaluate the feasibility of contrast-enhanced computed tomography for organ morphology and perfusion in five captive terrapins. Native scans were performed and afterwards an iodinated non-ionic contrast media was manually administered through the jugular vein catheter. Post-contrast CT scans were taken 20 (T_{20}), 60 (T_{60}) and 180 (T_{180}) seconds after the contrast medium administration. Maximum contrast enhancement of the kidneys and the liver was detected at T_{20} and T_{60}, respectively. The gall bladder content, the urinary bladder content and ovarian follicles were all without contrast enhancement in all five terrapins. Gall bladder wall thickness was 0.9 mm in all terrapins. Enhancement of the gall bladder wall in post-contrast studies was considered excellent, good or poor in two terrapins, two terrapins and one terrapin, respectively, with a mean score of 1.8 ± 0.84 over all contrast studies. Enhancement of the ureters in post-contrast studies was considered excellent in all terrapins in all contrast studies. Peak aortic enhancement was reached 20 seconds after contrast medium administration with the peak enhancement of 213.5 ± 41 HU in four terrapins and 560 HU in one terrapin. Peak hepatic vein enhancement after contrast medium administration was recorded 20 and 60 seconds in two and three terrapins, respectively. In conclusion, contrast-enhanced computed tomography proved to be a valuable method for clinical examination of the liver, gall bladder, kidneys, ureters, urinary bladder and ovarian follicles in red-eared terrapins.

Keywords: chelonians; computed tomography; contrast medium; organ perfusion; liver; kidneys

Lesions of different parenchymal organs in chelonian patients vary in severity and it is challenging for veterinarians to precisely evaluate the extent of tissue damage, and to provide an effective treatment. Physical examination is the standard step in clinical examination of reptile patients, but it has only limited value for making the exact diagnosis of organ disease. Haematology and plasma chemistry are feasible tools, but they are used for indirect control of organ function (Knotek et al. 2008; Campbell 2014). Studies using different methods of diagnostic imaging for diagnosis of organ function in chelonians have been published (Rubel and Kuoni 1991; DeShaw et al. 1996; Hernandez-Divers and Hernandez-Divers 2001; Hernandez-Divers and Lafortune 2004; Wilkinson et al. 2004; Silverman 2006; Gumpenberger 2011). Computed tomography (CT) is broadly applied as a diagnostic imag-

Supported by the Ministry of Education, Youth and Sports of the Czech Republic (Research Project IGA VFU 111/2015/FVL).

doi: 10.17221/73/2017-VETMED

ing method and is valuable in the characterisation of several diseases in chelonians (Gumpenberger and Henninger 2001; Gumpenberger 2002; Gumpenberger and Filip 2007; Marchiori et al. 2015; Spadola et al. 2016). The quantitative assessment of tissue density is expressed in Hounsfield units (HU, Kiefer and Pees 2011; Wyneken 2014; Marchiori et al. 2015). The slow respiratory rate in chelonians limits any possible artefacts caused by movement of lungs to minimum, but sedation or short-acting anaesthesia is necessary to prevent the risk of movement artefacts (Mans et al. 2013). Contrast-enhanced computed tomography (CECT) represents an advanced, powerful diagnostic tool to evaluate organ morphology and perfusion in captive reptiles. However, only a few studies have so far evaluated the use of CECT in reptiles (Gumpenberger and Filip 2007; Gumpenberger 2011; Nardini et al. 2014). The aim of the present study was to evaluate the feasibility of CECT in captive red-eared terrapins.

MATERIAL AND METHODS

Animals. The study was performed on five adult captive female red-eared terrapins (*Trachemys scripta elegans*) aged 12–15 years, with average body weight of 1.16 ± 0.25 kg. Terrapins were housed at the Avian and Exotic Animal Clinic and handled with the agreement of the Branch Commission for Animal Welfare of the Ministry of Agriculture of the Czech Republic (accreditation No. 45620/2008-17210, 45620/10001). The terrapins were kept in standard husbandry conditions in aquaria (74 cm × 67 cm × 88 cm) with a 12-hour day/12-hour night cycle provided by 100 W incandescent bulbs, and basking provided by UV/infrared lamps (D3 Basking Lamp 160 W, Arcadia, UK). Temperature in aquaria ranged from 25 °C to 30 °C, with water temperature ranging from 24 °C to 27 °C, and air humidity from 70 to 85%. All animals were fasted for 24 hours prior to the experiment. Complete physical examination of terrapins was performed before the procedure and the body weight of each terrapin was measured. Clinical examination and complete blood count showed no alterations and the terrapins were considered healthy. During the study, terrapins were housed individually in plastic containers placed on an electric heating pad (Bosch PFP 1031; Bosch, Czech Republic) at a temperature of 37.5 °C.

Analgesia and anaesthesia. Terrapins underwent CT imaging under inhalation anaesthesia with isoflurane. For analgesia, meloxicam (1 mg/kg, Metacam 5 mg/ml, Boehringer Ingelheim Vetmedica GmbH, Germany, Divers et al. 2010) and tramadol (10 mg/kg, Tramal 50 mg/ml, Fort Dodge Veterinaria S.A., Spain, Norton et al. 2013) were administered intramuscularly into the muscles of the left and right front legs. The anaesthesia was initiated with alfaxalone (5 mg/kg, Alfaxan 10 mg/ml, Vetoquinol, France) administered as a bolus intravenously to the subcarapacial sinus (Knotek 2014). A tracheal tube (14-gauge intravenous plastic catheter, Vasofix Safety, B. Braun Melsungen AG, Germany) was inserted and terrapins were kept under inhalation anaesthesia with a combination of 2–3% isoflurane (Aerrane, Baxter S.A., Lessines, Belgium) and oxygen (1 l/min) delivered by a small animal ventilator (SAV 03 Vetronic, UK) in a non-rebreathing circuit.

Jugular vein catheter. After disinfection with chlorhexidine spray (SkinMed, Cymedica Czech Republic), a small skin incision on the left or right side of the neck was made to visualise the jugular vein (*vena jugularis externa*). The intravenous catheter (22-gauge, Vasofix Safety, B. Braun Melsungen AG, Germany) was gently inserted into the jugular vein and secured to the skin with a suture (4-0 Caprolon, Resorba, Germany). Catheter insertion was performed by the same person (ZK) in all the animals. The ease of catheterisation of the jugular vein was graded subjectively on a scale from 1 to 5 (1 = excellent, catheter insertion was easily performed; 2 = good, catheter insertion was performed with small complications; 3 = satisfactory, catheter insertion had to be performed twice; 4 = difficult, catheter insertion had to be performed from the right side; 5 = impossible).

Computed tomography. CT of the terrapins was performed using a multidetector 16 slice scanner (LightSpeed, GE HealthCare, Milwaukee, USA). Transversal scans were obtained in a helical mode in a medium frequency algorithm (proprietary name standard), using 100 kV and automatic mA, with a range of 107–417. Slice thickness was set to 1.25 mm and spiral pitch factor was 0.9375. The terrapins were positioned in ventral recumbency with head and neck extended from the shell. Plain (precontrast) CT scans were performed and afterwards a dose of 2 ml/kg (800 mg I/kg) of an iodinated non-ionic contrast media (Iomeron 300, Bracco, Konstanz, Germany) was manually administered

doi: 10.17221/73/2017-VETMED

through the jugular catheter. Post-contrast CT scans were taken after the start of contrast medium administration in the following time intervals: 20 (T_{20}), 60 (T_{60}) and 180 (T_{180}) seconds. After transversal CT images were taken and stored, a multiplanar reconstruction was performed (proprietary GE Workstation v 4.4, GE HealthCare, Milwaukee, USA) for better visualisation. In each hepatic lobe, two regions of interest (ROI) were selected, totalling four ROIs per terrapin. Each selected ROI had an area of 25 ± 1 mm^2 to better exclude big vascular structures. Liver attenuation values in pre-contrast and post-contrast studies were determined. Attenuation values of the gall bladder were determined by the use of one ROI (area 25 ± 1 mm^2), gall bladder wall thickness was determined and gall bladder wall enhancement in post-contrast studies was subjectively estimated using a three-point scale (1–3). The global quality of enhancement was determined as excellent, good or poor by consensus when the gall bladder wall was clearly visualised (1), not clearly visualised (2) or when the gall bladder wall was without contrast enhancement (3), respectively. In each kidney parenchyma, one ROI (area 25 ± 1 mm^2) was selected in the central area and kidney attenuation values in pre-contrast and post-contrast studies were determined. Enhancement of the ureters was subjectively estimated using a three-point scale in post-contrast studies (as above), and attenuation values of the urinary bladder content were determined by the use of four ROIs (area 25 ± 1 mm^2) in pre-contrast and post-contrast studies. Attenuation values of the ovarian follicles were determined by using four ROIs (area 25 ± 1 mm^2) per terrapin in pre-contrast and post-contrast studies. For each follicle, a single size-adjusted ROI was used. In aorta one, ROI was selected (area of the aorta diameter) at the position where the left aorta connects the right aorta to form a single dorsal aorta and attenuation values were determined. In the right hepatic vein, one ROI was selected (area of the vein diameter) at the position where the right hepatic vein drains into the sinus venosus.

Follow-up. After the CT examination was done, the jugular catheter was withdrawn and the small skin incision was closed with a suture (4-0 Caprolon, Resorba, Germany) in an interrupted pattern. After recovery from anaesthesia, terrapins were kept overnight in terraria without water. All terrapins were released back into their aquaria on the day after the CT study.

Statistical analysis. All statistical tests were performed in the PC-based MedCalc software for Windows, version 14 (MedCalc Software, Ostend, Belgium). Descriptive statistics (mean ± SD, minimum, maximum) were used for analysis of data. The Friedman test with a subsequent Conover post-hoc test was used to assess the differences in attenuation values. A significance (α) level of 0.05 was used in this study.

RESULTS

The ease of intravenous catheter insertion was considered good with a mean score of 2.4 ± 0.89. In four terrapins, catheter insertion into the jugular vein was considered good, while in one terrapin (terrapin number 3) catheter insertion into the left jugular vein failed and the catheter had to be inserted into the right jugular vein.

Native density and density 20, 60 and 180 seconds after the start of intravenous administration of the contrast medium for the liver, gall bladder, the kidneys, the urinary bladder and ovarian follicles are summarised in Table 1. Maximum contrast

Table 1. Organ density (in Hounsfield units) after contrast medium administration in five red-eared terrapins. Values are presented as mean ± SD (min.–max.)

Organs	Native	T_{20}*	T_{60}**	T_{180}***
Liver	55.78 ± 11.66 (41–74)	94.12 ± 45.58 (42–165)	99.34 ± 18.36 (73–120)	88.56 ± 11.86 (73–104)
Gall bladder	35.08 ± 6.67 (29–46)	36.75 ± 4.48 (33–44)	37.19 ± 2.37 (35–40)	35.50 ± 3.81 (31–40)
Kidneys	39.50 ± 2.67 (35–44)	217.70 ± 35.78 (181–292)	168.5 ± 22.34 (143–208)	136.0 ± 6.76 (128–146)
Urinary bladder	1.98 ± 3.09 (–2–7)	0.97 ± 3.06 (–2–5)	0.78 ± 3.20 (–3–6)	0.60 ± 3.71 (–5–6)
Ovarian follicles	70.69 ± 6.79 (64–81)	71.81 ± 5.46 (67–81)	71.36 ± 6.74 (64–82)	70.48 ± 6.90 (66–82)

*T_{20} = 20 minutes after contrast medium administration; **T_{60} = 60 minutes after contrast medium administration; ***T_{180} = 180 minutes after contrast medium administration

doi: 10.17221/73/2017-VETMED

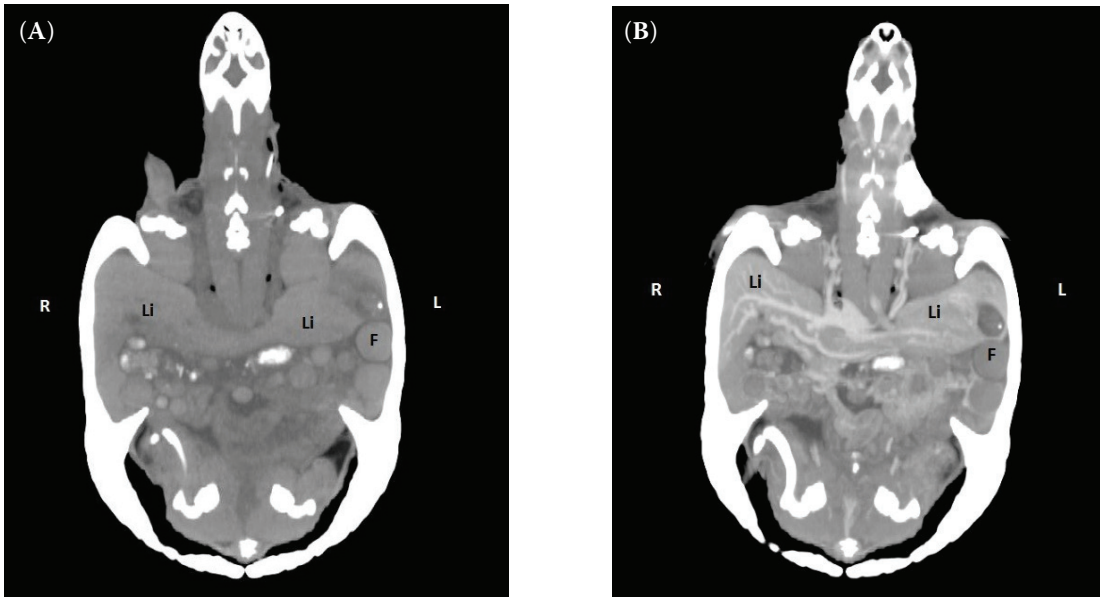

Figure 1. (**A**) Dorsal pre-contrast CT image (WW 400, WL 50) of the ventral half of the body at the level of the liver. (**B**) Dorsal post-contrast CT image (WW 400, WL 50) of the ventral half of the body. The large vessels within the liver parenchyma show strong enhancement

F = follicle, Li = liver

enhancement of the kidneys was detected 20 seconds after the contrast medium administration, while maximum contrast enhancement of the liver was detected 60 seconds after the contrast medium administration (Figure 1). Enhancement of the liver and kidney parenchyma was homogenous in all cases. There were statistically significant differences between each contrast study in liver and kidney parenchyma.

The gall bladder content, the urinary bladder content and ovarian follicles were all without contrast enhancement in all five terrapins. There were no statistically significant differences between any of the different contrast studies. It was not possible to differentiate the salpinx in any of the studies.

Gall bladder wall thickness was 0.9 mm in all terrapins. Enhancement of the gall bladder wall in

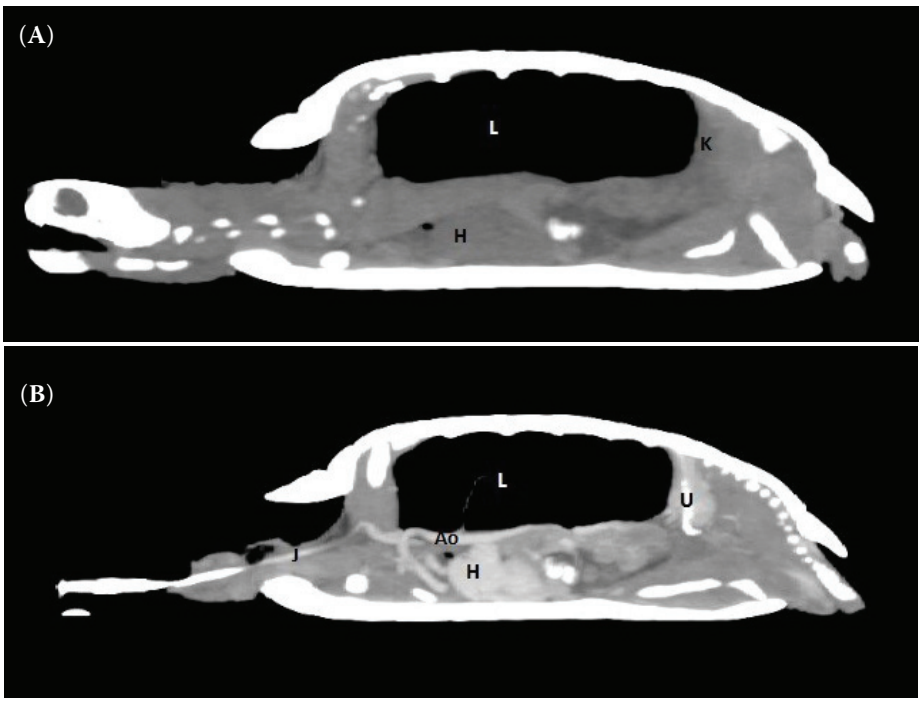

Figure 2. (**A**) Sagittal pre-contrast CT image (WW 400, WL 50). The kidneys (K) are poorly differentiable. (**B**) Sagittal early post-contrast images (WW 400, WL 50). The kidneys show excellent enhancement. The ureter (U) is visible in the kidney parenchyma. The large heart vessels show strong enhancement

Ao = aorta, H = heart, J = jugular vein, L = lung

doi: 10.17221/73/2017-VETMED

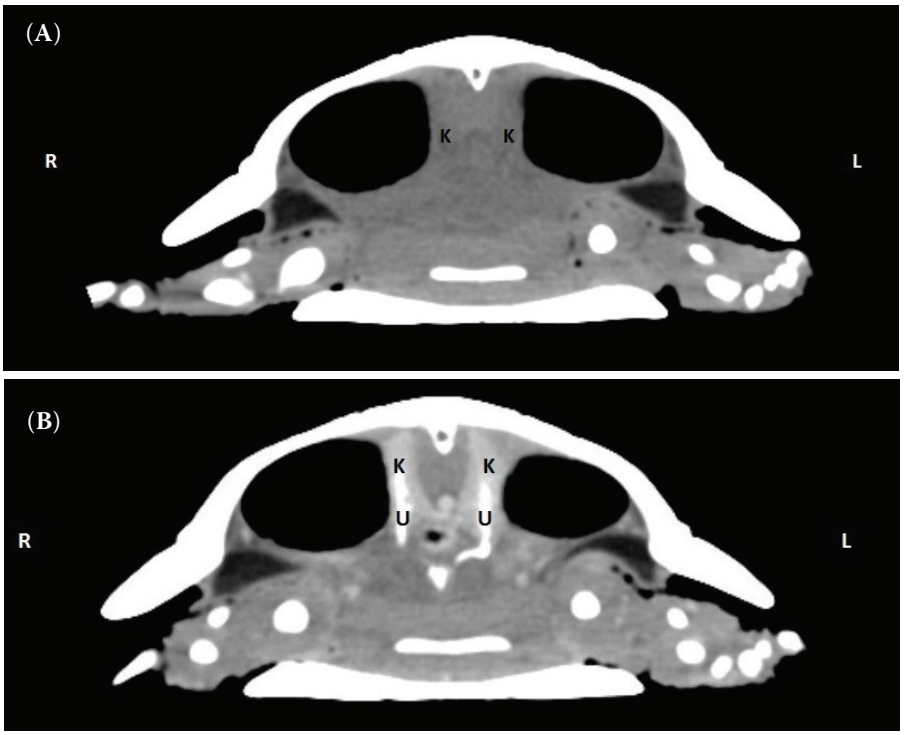

Figure 3. (**A**) Transverse pre-contrast CT image (WW 400, WL 50) at the level of the kidneys (K). (**B**) Transverse post-contrast CT image (WW 400, WL 50) at the level of the kidneys. The kidneys (K) show excellent enhancement. The ureters (U) are visible in the kidney parenchyma

post-contrast studies was considered excellent, good or poor in two terrapins, two terrapins and one terrapin, respectively, with a mean score of 1.8 ± 0.84 for all contrast studies. Enhancement of the ureters in post-contrast studies was considered excellent in all terrapins (Figures 2 and 3), whereas enhancement of the gall bladder wall in post-contrast studies was considered excellent in two terrapins only.

Peak aortic enhancement was reached 20 seconds after contrast medium administration with a peak enhancement of 213.5 ± 41 HU in four terrapins and 560 HU in one terrapin. Peak hepatic vein enhancement after contrast medium administration was recorded 20 and 60 seconds in two and three terrapins, respectively.

DISCUSSION

The jugular vein has been recommended for intravenous administration of contrast medium in chelonians (Gumpenberger 2011). In the present study, the ease of catheter insertion into the left jugular vein was considered good in four terrapins, while in one terrapin the catheter had to be replaced into the right jugular vein.

Chronic liver disease taking the form of steatosis to fibrosis, necrosis or neoplasia (Jacobson 2007), is a common problem in captive chelonians (McArthur 2004; McArthur et al. 2004; Campbell 2014; Marchiori et al. 2015). Some authors report that fatty liver disease decreases the organ density from 50–70 HU to –10––40 HU (Wilkinson et al. 2004; Kiefer and Pees 2011). Gumpenberger (2011) defined a fatty liver in the Hermann's tortoise as one with a density of lower than 20 HU. Marchiori et al. (2015) performed CT in 10 male red-footed tortoises. Mean radiographic attenuation values for the hepatic parenchyma were 11.2 ± 3.0 HU and seven male tortoises had values lower than 20 HU, which was considered compatible with hepatic lipidosis. From the practical point of view, it is important to know that the X-ray attenuation of the liver could be influenced by the age and species of chelonians involved in the study (Bonelli et al. 2013). The native density of the liver parenchyma in five female red-eared terrapins involved in the present study (55.78 ± 11.66 HU, 41–74 HU) was similar to that reported for healthy Hermann's tortoises (50–70 HU, Gumpenberger 2011) and young green sea turtles (60.09 ± 5.3 HU, Bonelli et al. 2013).

The attenuation values for the kidney parenchyma in five red-eared terrapins involved in the present study (39.50 ± 2.67 HU) were similar to findings published for Hermann's tortoises (Gumpenberger and Filip 2007; Gumpenberger 2011). The maximum enhancement of the kidney parenchyma was recorded 20 seconds after contrast medium administration.

doi: 10.17221/73/2017-VETMED

Similar findings were observed in adult Hermann's tortoises (Gumpenberger and Filip 2007).

In the present study, the native density of the gall bladder and urinary bladder was 35.08 ± 6.67 HU and 1.98 ± 3.09 HU, respectively. The attenuation values for ovarian follicles were similar to the ovarian follicle attenuation values for Hermann's tortoises reported by Gumpenberger (2011). The gall bladder content, the urinary bladder content and ovarian follicles were all without contrast enhancement after contrast medium administration in female red-eared terrapins. According to the authors' knowledge such measurements had not yet been performed in red-eared terrapins.

The enhancement of the ureters and the gall bladder wall was subjectively evaluated because of the small area for ROI measurement. Enhancement of the ureters in post-contrast studies was considered excellent in all terrapins, while enhancement of the gall bladder wall in post-contrast studies was considered excellent in two terrapins only.

The first visualisation of the contrast medium in the aorta of eight green iguanas was recorded 3.6 ± 0.5 seconds after contrast medium administration (Nardini et al. 2014). In red-eared terrapins, the peak aortic enhancement and the peak hepatic vein enhancement were recorded 20 seconds, and 20–60 seconds after contrast medium administration, respectively. Variations in density may be caused by differences in blood pressure, heart rate or hydration between individual tortoises or may result from different methods for contrast medium administration and the different reptile species that have been used. The main limitation of this study was that we did not use an automated bolus tracking method as in the study of Nardini et al. (2014). For intravenous contrast medium administration, the jugular vein or the coccygeal vein were recommended as sites of administration in chelonians (Gumpenberger 2011). In our study, the jugular vein was used in contrast with the study from Nardini et al. (2014). Differences in attenuation values may be expected when using different sites of administration due to the characteristic renal portal system in reptiles. To the best of the authors' knowledge, similar measurements have not yet been reported in red-eared terrapins or any other chelonian species. The authors are aware that the reported statistical analysis has limited value because of the low number of animals used in this study.

In conclusion, our results demonstrate that contrast-enhanced computed tomography is a valuable method for clinical examination of the internal organs in red-eared terrapins. CECT provided information about the blood supply of different parenchymal organs. This would allow early diagnosis of organ changes and could suggest corrective measures regarding treatment protocols, feeding and husbandry for captive chelonian species. CECT might also enable early detection of pathology in parenchymal organs not seen on plain CT scans. More studies with terrapins suffering from diseases affecting specific organs are needed.

Acknowledgement

The authors would like to thank Dr. Gumpenberger and Dr. Stehlik for their valuable comments.

REFERENCES

Bonelli MA, Oliveira DC, Costa LA, Forattini JG, Junior JL, Leite FL, Costa FS (2013): Quantitative computed tomography of the liver in juvenile green sea turtles (Chelonia mydas). Journal of Zoo and Wildlife Medicine 44, 310–314.

Campbell TW (2014): Clinical pathology. In: Mader DR, Divers SJ (eds): Current Therapy in Reptile Medicine and Surgery. Elsevier, St Louis. 70–92.

DeShaw B, Schoenfeld A, Cook RA, Haramati N (1996): Imaging of reptiles: a comparison study of various radiographic techniques. Journal of Zoo and Wildlife Medicine 27, 364–370.

Divers SJ, Papich M, McBride M, Stedman NL, Perpinan D, Koch TF, Hernandez SM, Barron GH, Pethel M, Budsberg SC (2010): Pharmacokinetics of meloxicam following intravenous and oral administration in green iguanas (Iguana iguana). American Journal of Veterinary Research 71, 1277–1283.

Gumpenberger M (2002): Computed tomography (CT) in chelonians. Proceedings of the 9th Annual Conference of Association of Reptilian and Amphibian Veterinarians. 41–43.

Gumpenberger M (2011): Chelonians. In: Schwarz T, Saunders J (eds): Veterinary Computed Tomography. Wiley-Blackwell, Oxford. 533–544.

Gumpenberger M, Henninger W (2001): The use of computed tomography in avian and reptile medicine. Seminars in Avian and Exotic Pet Medicine 10, 174–180.

doi: 10.17221/73/2017-VETMED

Gumpenberger M, Filip T (2007): Computed tomography and use of intravenous contrast media in imaging chelonian kidneys. Proceedings of the 14th Annual Conference of Association of Reptilian and Amphibian Veterinarians. 5.

Hernandez-Divers SM, Hernandez-Divers SJ (2001): Diagnostic imaging of reptiles. In Practice 23, 370–391.

Hernandez-Divers SJ, Lafortune M (2004): Radiology. In: McArthur S, Wilkinson R, Meyer J, Innis C, Hernandez-Divers SJ (eds): Medicine and Surgery of Tortoises and Turtles. Blackwell Scientific Publications, London. 195–212.

Jacobson ER (2007): Infectious Diseases and Pathology of Reptiles. CRC Press, Boca Raton. 716 pp.

Kiefer I, Pees M (2011): Computed tomography (CT). In: Krautwald-Junghanns ME, Pees M, Reese S, Tully T (eds): Diagnostic Imaging of Exotic Pets. Schlutersche Vrlg, Hannover. 358–367.

Knotek Z (2014): Alfaxalone as an induction agent for terrapins and tortoises. Veterinary Record, doi:10.1136/vr.102486.

Knotek Z, Dorrestein GM, Knotkova Z (2008): Chronic liver disease. What we know about it? Proceedings Abstracts, 5 Congres Veterinaire International sur les animaux sauvages et exotiques. Paris March 20.–22. 2008. 33–34.

Mans C, Drees R, Sladky KK, Hatt JM, Kircher PR (2013): Effects of body position and extension of the neck and extremities on lung volume measured via computed tomography in red-eared slider turtles (Trachemys scripta elegans). Journal of American Veterinary Medical Association 243, 1190–1196.

Marchiori A, da Silva IC, de Albuquerque Bonelli M, de Albuquerque Zanotti LC, Siqueira DB, Zanotti AP, Costa FS (2015): Use of computed tomography for investigation of hepatic lipidosis in captive Chelonoidis carbonaria (Spix, 1824). Journal of Zoo and Wildlife Medicine 46, 320–324.

McArthur S (2004): Problem-solving approach to common diseases of terrestrial and semi-aquatic chelonians. In: McArthur S, Wilkinson R, Meyer J, Innis C, Hernandez-Divers S (eds): Medicine and Surgery of Tortoises and Turtles. Blackwell Scientific Publications, London. 309–377.

McArthur S, McLellan L, Brown S (2004): Gastrointestinal system. In: Girling SJ, Raiti P (eds): Manual of Reptiles. 2nd edn. British Small Animal Veterinary Association, Quedgeley. 210–229.

Nardini G, Di Girolamo N, Leopardi S, Paganelli I, Zaghini A, Origgi F, Vignoli M (2014): Evaluation of liver parenchyma and perfusion using dynamic contrast-enhanced computed tomography and contrast-enhanced ultrasonography in captive green iguanas (Iguana iguana) under general anesthesia. BMC Veterinary Research 10, doi: 10.1186/1746-6148-10-112.

Norton T, Cox S, Kaylor M, Hupp A, Thomas R, Nelsen S, Sladky KK (2013): Pharmacokinetics of tramadol and O-desmethyltramadol in loggerhead sea turtles (Caretta caretta). Proceedings of the 33rd ISTS Symposium on sea turtle biology and conservation. February 2.–8. 2013. 20–21.

Rubel A, Kuoni W (1991): Radiology and imaging. In: Frye FL (ed.): Biomedical and Surgical Aspects of Captive Reptile Husbandry. 2nd edn. Krieger Publishing, Melbourne. 185–208.

Silverman S (2006): Diagnostic imaging. In: Mader DR (ed.): Reptile Medicine and Surgery. 2nd edn. Saunders Elsevier, St Louis. 471–489.

Spadola F, Barillaro G, Morici M, Nocera A, Knotek Z (2016): The practical use of computed tomography in evaluation of shell lesions in six loggerhead turtles (Caretta carettta). Veterinarni Medicina 61, 394–398.

Wilkinson R, Hernandez-Divers S, Lafortune M, Calvert I, Gumpenberger M, McArthur S (2004): Diagnostic imaging. In: McArthur S, Wilkinson R, Meyer J, Innis C, Hernandez-Divers S (eds): Medicine and Surgery of Tortoises and Turtles. Blackwell Scientific Publications, London. 187–238.

Wyneken J (2014): Computed tomography and magnetic resonance imaging. In: Mader DR, Divers SJ (eds): Current Therapy in Reptile Medicine and Surgery. Elsevier, St Louis. 93–106.

Received: May 25, 2017
Accepted after corrections: October 18, 2017